

Characterization, Comparative Study, and Kinetic Modeling of Waste Plastic and Biomass Blend for Bio-Fuel Application

Mahlet K. Tabour^{1,*}, A.Venkata Ramayya¹ and Million M. Afessa^{1,2}

¹ Faculty of Mechanical Engineering, Jimma Institute of Technology (JIT), Jimma University, Ethiopia

² Department of Chemistry, Material, and Chemical Engineering, Politecnico di Milano, Italy

Corresponding author: mahletemu8@gmail.com

ABSTRACT

Pyrolysis of plastic Waste is the best way to manage the waste while producing biofuels which can be improved to replace diesel. However, thermal pyrolysis of plastic has some drawbacks, namely the high decomposition temperature. Co-pyrolytic processes have drawn much attention for offering an alternate method of disposing of and turning waste plastic and lignocellulosic biomass into high-value-added products. In this work, pine sawdust (SD) co-pyrolysis with Polypropylene (PP) and polystyrene (PS) was investigated, which resulted in a decrease in the decomposition temperature. The major goal of this work is to better understand the co-pyrolysis of biomass and plastic waste by applying two model-fitting techniques (Criado's and Coats-Redfern). Co-pyrolysis behavior of pine sawdust, waste plastics, and their blends was characterized using a thermogravimetric analyzer (TGA). The data obtained from TGA reveals the decomposition behavior of the materials involved and their synergistic effect. Seven different co-pyrolysis tests were conducted using (TGA) at a heating rate of 20°C/min for different binary and ternary mixed compositions of the samples. The values of the activation energy (E_a) and pre-exponential factor (A_0) of waste plastics (PP and PS) and pine sawdust (SD) decomposition were found to be 111.4, 110.46, and 48.78 kJ/mol, respectively. Adding pine sawdust to plastic decreased the activation energy of the plastic decomposition reaction to 99.35 kJ/mol. This positive synergy shows that the co-pyrolysis of plastic with biomass decrease the plastic's decomposition temperature and increase the biomass sample's conversion rate.

Keywords: blended fuel performance, Co-pyrolysis, nonconventional fuel, Renewable fuel, waste to energy

INTRODUCTION

Solid waste management is among the most persistent global concerns confronting environmental sustainability. Now, there are 2.01 billion tons of waste produced annually in the world, and by 2050, that number is expected to rise to 3.4 billion (Gin et al., 2021). The two main components of solid waste are biomass and plastic garbage. According to estimates, Ethiopia produces 0.6 to 1.8 million tons of waste annually in rural regions and 2.2 to 7 million tons annually in urban areas (Teshome, 2021). Thus, there is a significant need to handle these solid wastes and reduce their environmental impact adequately.

On the other hand, the depletion of fossil fuel resources and environmental concerns such as global warming and air pollution are becoming a problem. So researchers are looking for renewable fuels to replace fossil-derived energy sources (Dyer et al., 2021; Stančin et al., 2021; X. Wang et al., 2019). Plastic and biomass wastes are the primary sources of energy that can produce biofuels to replace fossil fuels (Z. Wang et al., 2021). Many strategies have been proposed to utilize waste plastics, especially for energy and fuel production, and to avoid resource wastage and environmental pollution. Therefore, promoting the principle of reducing, reusing, and recycling, and distributed generation/production has to practice to design sustainability which relies on decarbonization, dematerialization (conservation of depletable materials and zero waste philosophy). Pyrolysis is the most effective method of addressing these issues.

In the absence of oxygen, pyrolysis is the heat decomposition of organic molecules to create liquids, solids, and non-condensable gases (X. Wang et al., 2019). It is crucial to comprehend the behavior and evolution of processes that combine plastic pyrolysis with biomass. Solid organic biomass has a higher ash and oxygen content than waste plastics but less volatiles, hydrogen, and calorific content. Around 14 mass percent of the hydrogen in Polypropylene (PP) plastics. As a result, these plastics may contribute hydrogen to biomass co-pyrolysis, increasing liquid production and enhancing oil quality (Ozsin, 2018) (Zhang et al., n.d.) (Burra & Gupta, 2018) (Reactor et al., 2016). The course of reaction progression must be made clear through the kinetic study of pyrolysis,

and process variables' effects on reaction rate must be identified. The main objectives of kinetic analysis are to determine the decomposition mechanism(s) and calculate the parameters of the Arrhenius equation (Xing et al., 2019) (El-Sayed & Mostafa, 2015). When TGA data is combined with numerical modeling, it is possible to gain crucial insights into the behavior of biomass during pyrolysis and link it with the parameters of separated feedstock from heat and mass transfer processes (Afessa et al., 2022). Using a thermogravimetric analyzer (TGA) at 60 K/min, Dubdub et al. (Dubdub & Al-Yaari, 2020) investigated seventeen co-pyrolysis tests for different compositions of LDPE, HDPE, PP, and PS. Criado and Coats-Redfern techniques were used. The co-pyrolysis of mixed polymers was delayed. The co-pyrolysis of several polymer blends had an evident synergistic impact. H. Stanin et al. (Stančin et al., 2021) look into the co-pyrolysis and synergistic impact studies of Sawdust (SD) and Polystyrene (PS) mixes for the production of high-quality bio-oils. TGA was used, and a different blend ratio was used for the co-pyrolysis. At a PS ratio of 75%, the maximum liquid yield (83.86%) was obtained. The quality and output of the bio-oil are both greatly improved by PS, according to the results. Limited work is reported in the co-pyrolysis of mixed Polypropylene and Polystyrene (PP and PS) plastics and biomass (Pine sawdust wood). It needs to be further investigated to improve the bio-oil yield. This study aims to provide feasible and advantageous means for the efficient and clean disposal of plastic waste to maximize synergistic benefits in waste disposal, energy recovery, and incorporating value-added products within this scope.

MATERIAL AND METHODS

Sample Preparation

For this experiment, waste plastics and wood sawdust were used as feedstock. Pine sawdust was gathered from Jimma City, located in south-western Oromia (latitude and longitude of 7°40'N 36°50'E). This experiment used two types of plastics. As depicted in Figure 1, colorless disposable polystyrene (PS) cups and Polypropylene (PP) drinking straw plastics are utilized.

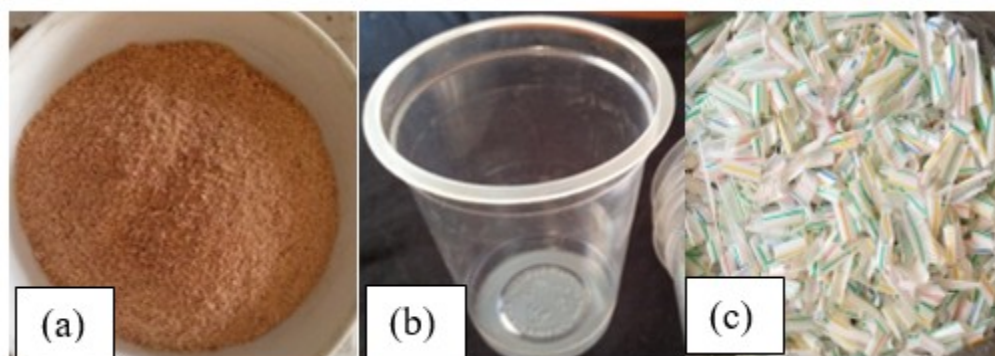


Figure 1. (a) Disposable Polystyrene cup; (b) Shredded Polypropylene plastic straw, and (c) Grinding machine. High moisture feedstock results in high water content in bio-oil. To remove the moisture content, Sawdust (SD) was dried in a furnace at 105°C for 24 hours. After drying, it was ground and sieved to a sample

size of less than or equal to 0.5 mm. The plastic was crushed and sieved to a size less than or equal to 0.7mm.

Proximate and ultimate analysis

Proximate analysis

Volatile matter and ash content are the major factors

Table 1. Proximate analysis of feedstock.

Sample	Moisture content [%]	Volatile matter [%]	Fixed carbon [%]	Ash [%]
Pine sawdust SD	7.08	73.29	18.37	1.26
Polystyrene PS	0.16	99.37	0.21	0.26
Polypropylene PP	0.10	98.94	0.16	0.80

Ultimate analysis

The ultimate analysis determines the samples' weight fractions of non-mineral major elements (i.e., carbon, hydrogen, nitrogen, oxygen, and sulfur). Elemental analysis or ultimate analysis of the samples (Sawdust, Polypropylene, and Polystyrene) were determined from literature reviews as shown in Table 2 (Phyllis2, 2022).

Table 2: Elemental analysis of Pine sawdust, Polypropylene, and Polystyrene (Phyllis2, 2022).

Element	Sawdust t [wt.%]	Polypropylene e [wt.%]	Polystyrene e [wt.%]
Carbon	47.43	85.39	92.70
Hydrogen	5.58	14.28	7.90
Oxygen	39.79	0.19	0.00
Nitrogen	0.09	-	-
Sulfur	0.01	-	-
Total	99.99	100.04	100.60

Thermogravimetric analysis

The ground samples (PP, PS, and SD) of less or equal to 0.7 mm particle size were weighted to an average sample mass of 10 mg; after weighing the sample, it was placed in an Al₂O₃ crucible. The blend ratio of the feedstock is given in Table 3. Pyrolysis of PP, PS, SD, and its binary and trinary blend (PP/PS/SD) at a constant heating rate of 20°C/min was performed using a Thermogravimetric analyzer (NETZSCHSTA 409 PC/PG). Thermal decomposition experiments were conducted under Argon gas (Ar) flowing at 60ml/min rate of purge gas. The temperature ranges from 30°C to 700°C.

Table 3. Experimental matrix (mixing ratio of samples).

Test numbers	Weight [%]		
	PP	PS	SD
Test 1	100	0	0
Test 2	0	100	0
Test 3	0	0	100
Test 4	25	75	0
Test 5	0	75	25
Test 6	75	0	25
Test 7	25	50	25

Kinetic Modeling

In this paper, one model-fitting single heating rate method, the Coats-Redfern equation, is used to calculate the kinetic parameters (activation energy and pre-exponential factor).

influencing the liquid oil yield in pyrolysis (Hasan et al., 2019). Proximate analysis is a technique used to measure a sample's chemical properties depending on the volatile matter, moisture content, fixed carbon, and ash content. In this study, the proximate analysis results of the samples are presented in Table 1 below.

Coats-Redfern Method

The Coats-Redfern method is one of the single heating rate methods used to calculate the kinetic parameters. Reaction conversion is typically expressed as shown in Eq.1 below (Singh et al., 2021; Li et al., 2021):

$$\alpha = \frac{w_0 - w_t}{w_0 - w_f} \quad (1)$$

Where w_t is the mass of the feedstock at a specific reaction time, w_0 and w_f are the initial and final mass of the feedstock at the investigated temperature desired and final reaction time, respectively?

The Coats-Redfern approach, an integral model-fitting method, estimates the temperature integral using an asymptotic series expansion. This method's final equation is shown in Eq. 2 (Dubdub & Al - yaari, 2020):

$$\ln \left[\frac{g(\alpha)}{T^2} \right] = \ln \left[\frac{A_0 R}{\beta E_a} \right] - \frac{E_a}{RT} \quad (2)$$

For the constant heating rate (β) and selected reaction mechanism ($g(\alpha)$), plotting $\ln[g(\alpha)/T^2]$ against $1/T$ will give a straight-line correlation with slope and intercept of $-E_a/R$, and $\ln(A_0 R/\beta E_a)$, respectively. Linear regression is used to calculate the kinetic parameters. The slope and the intercept can be used to calculate E_a and A_0 .

Criado's master plot

Criado's equation can be expressed as follows (Eq. 3) (Singh et al., 2021):

$$\frac{Z(\alpha)}{Z(0.5)} = \frac{f(\alpha)g(\alpha)}{f(0.5)g(0.5)} = \left(\frac{T_\alpha}{T_{0.5}} \right) \left(\frac{d\alpha}{dt} \right)_\alpha \quad (3)$$

Where: $f(\alpha)$ Concentration-dependent term (see Table 4), $g(\alpha)$ Concentration-dependent term (see Table 4), T_α : The temperature at conversion α , $T_{0.5}$: The temperature at conversion $\alpha = 0.5$, $\left(\frac{d\alpha}{dt} \right)_\alpha$:

Conversion change with time at conversion α , $\left(\frac{d\alpha}{dt} \right)_{0.5}$: Conversion changes with time at conversion $\alpha = 0.5$. The left-hand side of Eq.3 ($f(\alpha)g(\alpha)/f(0.5)g(0.5)$) is referred to as a reduced theoretical curve ($Z(\alpha)/Z(0.5)$), and it is characteristic to each reaction mechanism, whereas the right-hand side can be determined from experimental data. An iterative comparison of these two sides will reveal which exact kinetic model best describes the reaction (Dhyani & Bhaskar, 2018; Dubdub & Al-Yaari, 2020).

Table 4: Common solid-state thermal reaction mechanism (Dubdub & Al-Yaari, 2020)

Reaction Mechanism	$f(\alpha)$	$g(\alpha)$
First-order reaction (F1)	$1 - \alpha$	$-\ln(1 - \alpha)$
Second-order reaction (F2)	$(1 - \alpha)^2$	$[1/(1 - \alpha)] - 1$
Third-order reaction (F3)	$(1 - \alpha)^3$	$\{[1/(1 - \alpha)^2] - 1\}/2$
One-dimensional diffusion (D1)	$1/(2\alpha)$	α^2
Two-dimensional diffusion (D2)	$1/[-\ln(1 - \alpha)]$	$(1 - \alpha) \ln(1 - \alpha) + \alpha$
Three-dimensional diffusion (D3)	$3/\{2[1 - (1 - \alpha)^{1/3}]\}$	$[1 - (1 - \alpha)^{1/3}]^2$
Avrami-Erofeev (A2)	$2(1 - \alpha)[-\ln(1 - \alpha)]^{1/2}$	$[-\ln(1 - \alpha)]^{1/2}$
Avrami-Erofeev (A3)	$3(1 - \alpha)[-\ln(1 - \alpha)]^{2/3}$	$[-\ln(1 - \alpha)]^{1/3}$
Avrami-Erofeev (A4)	$4(1 - \alpha)[-\ln(1 - \alpha)]^{3/4}$	$[-\ln(1 - \alpha)]^{1/4}$
Phase boundary – one dimension (R1)	1	A
Contracting cylinder (R2)	$2(1 - \alpha)^{1/2}$	$1 - (1 - \alpha)^{1/2}$
Contracting sphere (R3)	$3(1 - \alpha)^{1/3}$	$1 - (1 - \alpha)^{1/3}$
Power law (P2)	$2\alpha^{1/2}$	$\alpha^{1/2}$
Power law (P3)	$3\alpha^{2/3}$	$\alpha^{1/3}$
Power law (P4)	$4\alpha^{3/4}$	$\alpha^{1/4}$

RESULTS AND DISCUSSION

In this section pyrolysis of feedstock and their blends were observed by a thermogravimetric analyzer (TGA). Criado's master plot is used to determine the suitable reaction mechanism. Whereas the kinetic parameters are calculated using the Coates-Redfern equation. Finally, the results are compared with the previous results from the literature.

TGA results

The differential thermogravimetric (DTG) curves can be divided into three groups. The first segment shows the removal of moisture, the second shows the highest devolatilization, which is the active pyrolysis stage, and the third is a continuous moderate devolatilization, which typically leaves a higher proportion of solid residue (El-sayed & Mostafa, 2015). The DTG curve, the TG curve's first derivative, shows the mass change over time along the temperature program.

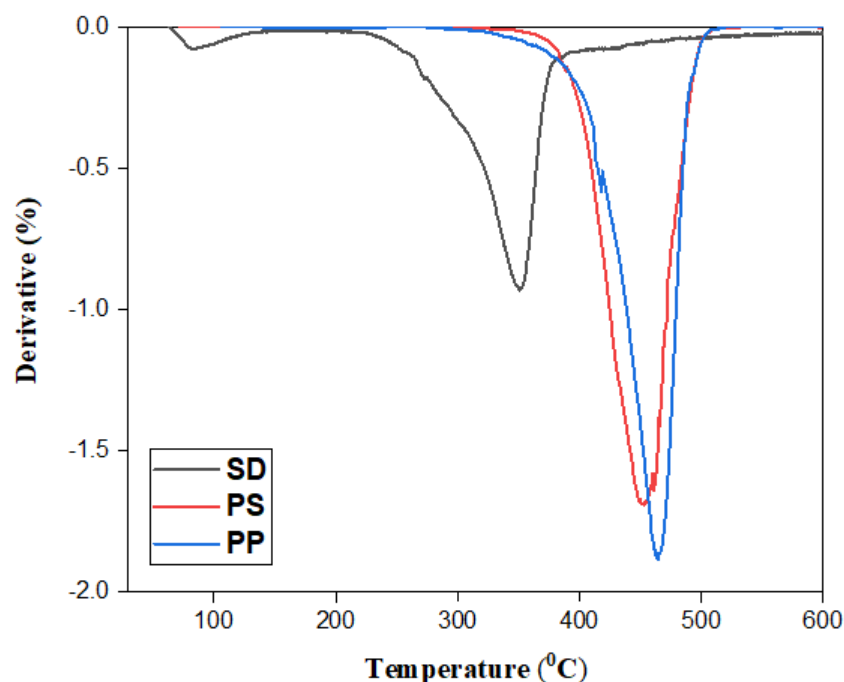


Figure 2. Comparison DTG curve of pure samples.

Sawdust begins to break down at a lower temperature (235°C), and Polymers (PP and PS) begin at 370°C and 359°C, respectively. Finally, PS plastic decomposed almost 99% (less than 2%), PP decomposed 96% with less than 5% residue, and SD

decomposed approximately 65%. As shown in the DTG curve, Figure 2, the maximum decomposition temperatures of SD, PS, and PP were 350°C, 452°C, and 464°C, respectively

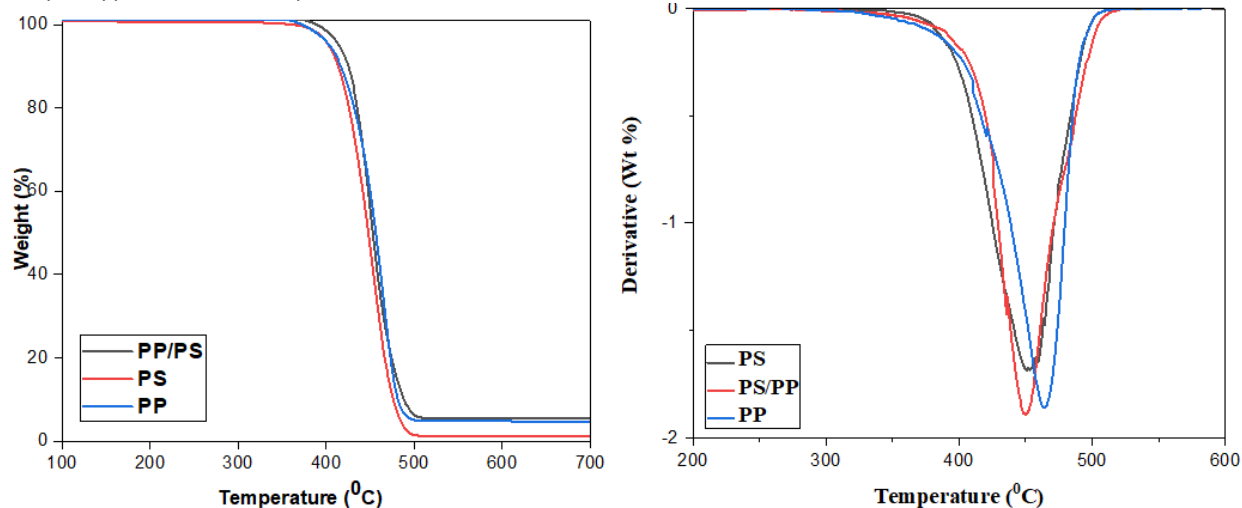


Figure 3. Comparison of TGA and DTG curve of PP, PS, and PP/PS.

The mixed plastics (PP/PS) decompose at 386–522 °C, figure 3. The onset temperature is greater than that of pure plastics. Up to 522, weight loss was 94.5%, and the residue was 5.5%. The maximum decomposition temperature of PP/PS is in between the pure polymers decomposition temperature; in the following sequence, the decomposition temperature of PS < PS/PP < PP. The PS/PP samples at different

compositions have T_{peak} between pure PS and PP, as shown in Figure 3. The decrease in the decomposition temperature is another proof of the observed synergistic effect, which can be due to the transfer of a hydrogen atom from the less stable polymer to the other during the pyrolysis process (Dubdub & Al-Yaari, 2020).

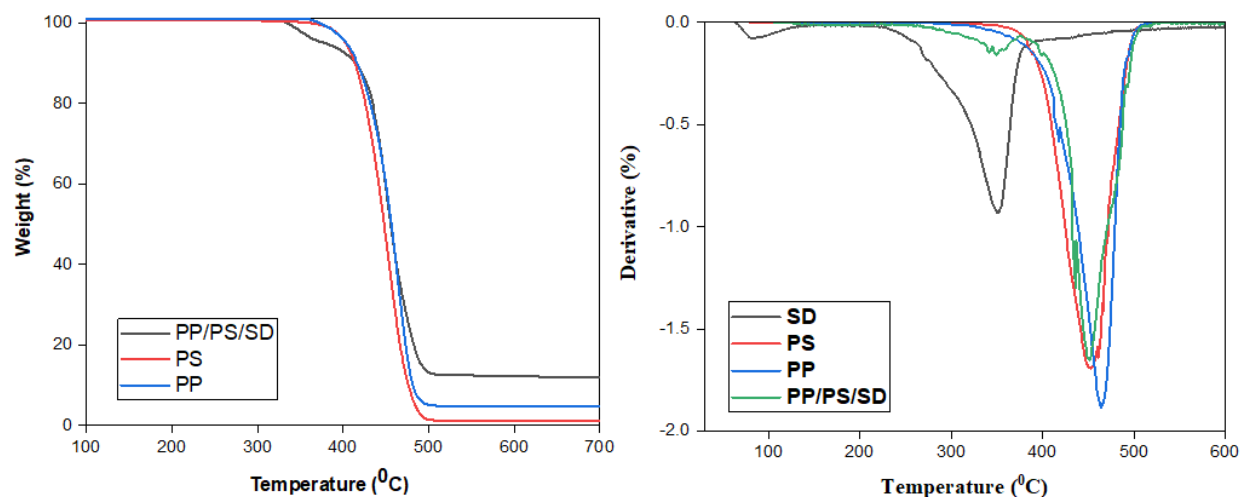


Figure 4. Comparison graph of pure samples and ternary mixture

Two decomposition ranges were found for the ternary mixture (PP/PS/SD), as shown in Figure 4. The decomposition profile of pure PP, PS, and PP/PS/SD mixture are compared. The onset temperature of the mixture is less than that of the pure plastics. The maximum decomposition temperature is also decreased to 450°C, which shows the synergistic effect of decreasing the decomposition temperature of plastics and the amount of biomass residue.

Determination of Reaction Mechanisms and Kinetic Parameters

The best reaction mechanism is selected depending on Criado's master plot. The theoretical curve that

best fits the experimental curve is selected. As shown in figure 5, Diffusion Model (D1), Geometric Contraction Model (R1), and Power Law Models (P2, P3, and P4) reaction mechanisms equally fit with the experimental value.

The Coats-Redfern model was used to determine the kinetic parameters activation energy and pre-exponential factor (E and A_0). After determining the optimal reaction mechanism from Criado's plot and selecting the $g(\alpha)$ from Table 4, the kinetic parameters are calculated for each test by plotting $\ln[g(\alpha)/T^2]$ versus $1/T$ as shown in Figure 6.

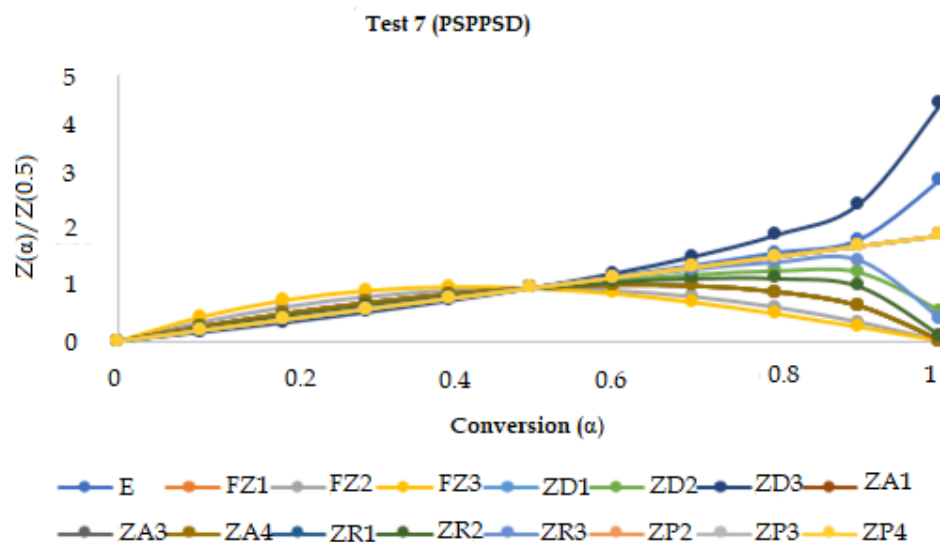


Figure 5. Criado's model master plots of biomass, polymers, binary and ternary mixtures.

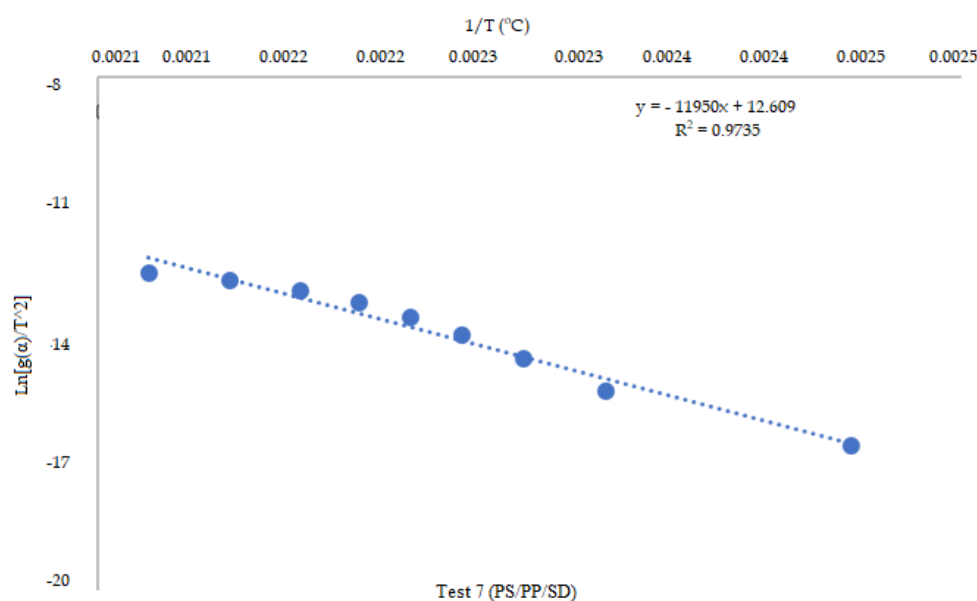


Figure 6. Plots of Coats-Redfern model.

The E_a values obtained by the A2, A3, and A4 reaction mechanisms were eliminated because they significantly differed from the predicted and published results. The E_a , $\ln(A_0)$, and R^2 values for each test are shown in Table 5. Depending on the reaction mechanism model used, E_a values range from 48.78 to 104.68 kJ/mol. As illustrated in Table 5, the main controlling reaction mechanism is one-dimensional diffusion (D1). The activation energy and pre-exponential factor were calculated using linear regression, as shown in Figure 6. The highest R^2 value among reaction orders that have been equally fitted is chosen, and the outcomes are displayed in Table 5.

Other research supports the idea that the co-pyrolysis of plastic and pine sawdust reduces the decomposition temperature (Xue et al., 2017). Moreover, the co-pyrolysis of plastic and biomass has a synergistic effect on lowering the activation energy of plastics, which lowers the mixture's maximum degradation temperature and onset temperature (Stančin et al., 2021). Table 5 demonstrates how the activation energy of the biomass and plastic mixture decreased. The interaction between pine sawdust and waste plastics during the decomposition reaction led to these outcomes.

Table 5. Kinetic parameters of the pyrolysis of biomass, polymers, and their mixtures obtained by the Coats-Redfern model and previous results from the literature.

Test No.	Kinetic parameters			E/log [A ₀]	Reaction mechanisms
	Ea [kJ/mol]	Ln(A ₀) [min ⁻¹]	R ²		
1.(PP)	111.4	28.24	0.9935	9.086	One dimensional diffusion(D1)
2.(PS)	110.46	28.36	0.9640	8.97	One dimensional diffusion(D1)
3.(SD)	48.78	13.9	0.9958	8.089	Three-dimensional diffusion(D3)
4.(PP/PS)	76.29	18.5	0.9658	9.5	Phase boundary-one dimension(R1)
5.(PS/SD)	80.26	20.16	0.9806	9.137	One dimensional diffusion(D1)
6.(PP/SD)	104.68	25.37	0.9962	9.5	One dimensional diffusion(D1)
7.(PP/PS/SD)	99.35	24.99	0.9735	9.15	One dimensional diffusion(D1)

Kinetic parameter results from related literature					
Sample types (Mixing ratio)	E [kJ/mol]	Ln(A ₀) [min ⁻¹]	Temp. range(°C), T _{peak} , β [°C/min]	Models used	References
PS/PP (70/30)	193	31.41	30-850, 60	Coats-Redfern	(Dubdub & Al-Yaari, 2020)
PP/PS (70/30)	179	29.4	30-850, 60	Coats-Redfern	(Dubdub & Al-Yaari, 2020)
PP/PS (50:50)	161	-	27-800	Coats-Redfern	(Dubdub & Al-Yaari, 2021)
PP(100)	187	-	30-1000	Coats-Redfern	(Aboulkas et al., 2010)
PP/SD(50/50)	198.4-263.6	-	30-600,5-40	Friedman	(Han et al., 2014)

CONCLUSION

Co-pyrolysis behaviors of SD, PP, PS, and their blend were studied. Pyrolysis processes were performed in a thermogravimetric analyzer (TGA) for pure (PP, PS, and SD) and its mixed samples to investigate the decomposition behavior. The TGA results show that the maximum SD, PP, and PS conversion for the given operating conditions are 65%, 95%, and 99%, respectively. It also shows that the maximum decomposition temperature of biomass and plastic blend(PP/PS/SD) is 450°C. The data obtained from TGA was used to determine the kinetic parameters (activation energy and pre-exponential factor) using two model fitting (Criado and Coats Redfern)

approaches. The kinetics of the thermal degradation of waste plastics (PP, PD) and pine sawdust(SD) biomass was determined from experiments at a heating rate of 20°C/min. Two model-fitting methods, Coats-Redfern and Criado methods, were successfully utilized to predict the reaction mechanism and calculate the activation energy for the thermal degradation of plastics and biomass waste. The activation energy values ranged from 48.78 to 111.4 kJ/mol depending on the adequately selected model reaction mechanism. Finally, it is observed that the pyrolysis reaction models of mixed plastic and biomass feedstock can be described by the "One-dimensional diffusion(D1)" model.

Nomenclature		Units	
T	Temperature [K, °C]	PS	Polystyrene
P	Pressure [Kpa]	SD	Pine Sawdust
α	Conversion [%]	HHV	Higher Heating Value
t	Time [Sec]	PP	Polypropylene
A ₀	Pre-exponential factor [min ⁻¹]	TGA	Thermogravimetric analyzer
E _a	Activation energy [kJ/kmol]	DTG	Differential Thermogravimetric
R	Universal gas constant [J mol ⁻¹ K ⁻¹]		
r	Reaction rate	°C	Degree Celsius
β	Heating rate [K/min]	K	Kelvin
f(α)	Differential form of the α-dependent part of the rate equation	h	hour
g(α)	The integral form of the α-dependent part of the rate equation	Kg	Kilogram
n	Order of the pyrolysis reaction	KJ	Kilo Joule
w _t	The mass of the feedstock at a specific reaction time [g]	min	Minute
w ₀	The initial mass of the feedstock at the investigated temperature desired	g	Gram
w _f	The final mass of feedstock at a final reaction time[g]	KPa	Kilopascal
		J	joule

ACKNOWLEDGMENTS

The authors gratefully acknowledge Jimma Institute of Technology Laboratory for the experimental work and the KFW (project No. 51235) through EXIST Project being implemented at Jimma Institute of Technology for the financial support.

REFERENCES

- Aboulkas, A, El harfi, K and El Bouadili, A. 2010. Thermal degradation behaviors of polyethylene and Polypropylene. Part I: Pyrolysis kinetics and mechanisms. *Energy Conversion and Management*. 51(7): 1363-1369.
- Afessa, MM, Debiagi, P, Ferreiro, AI, Mendes, MAA, Faravelli, T and Ramayya, AV. 2022.

- Experimental and modeling investigation on pyrolysis of agricultural biomass residues: Khat stem and coffee husk for bio-oil application. *Journal of Analytical and Applied Pyrolysis*. 162: 105435. <https://doi.org/10.1016/j.jaap.2022.105435>
- Burra, KG & Gupta, AK.(2018). Kinetics of synergistic effects in co-pyrolysis of biomass with plastic wastes. *Applied Energy* 220: pp. 408–418. <https://doi.org/10.1016/j.apenergy.2018.03.117>
- Dhyani, V and Bhaskar, T. 2018. Kinetic Analysis of Biomass Pyrolysis. In *Waste Biorefinery*. Elsevier B.V. <https://doi.org/10.1016/B978-0-444-63992-9.00002-1>
- Dubdub, I and Al-yaari, M. 2020. *Pyrolysis of Mixed Plastic Waste : I . Kinetic Study*.
- Dubdub, I and Al-Yaari, M. (2020). Pyrolysis of mixed plastic Waste: I. kinetic study. *Materials*. 13(21): 1–15.
- Dubdub, I and Al-Yaari, M. 2021. Thermal behavior of mixed plastics at different heating rates: I. pyrolysis kinetics. *Polymers*. 13(19). <https://doi.org/10.3390/polym13193413>
- Dyer, AC, Nahil, MA, and Williams, PT. 2021. Catalytic co-pyrolysis of biomass and waste plastics as a route to upgraded bio-oil. *Journal of the Energy Institute*. 97: 27–36.
- El-sayed, SA and Mostafa, ME. 2015. Thermal Analysis and Kinetic Parameters Determination of Biomass Pyrolysis Using (TGA / DTG) and (DTA) at different heating rates , accepted for publication in *Waste and Biomass Valor ... Kinetic Parameters Determination of Biomass Pyrolysis Fuels Usi. Waste and Biomass Valorization*. 6(3): 401–415. <https://doi.org/10.1007/s12649-015-9354-7>
- Gin, AW, Hassan, H, Ahmad, MA, Hameed, BH and Mohd Din, AT. 2021. Recent progress on catalytic co-pyrolysis of plastic waste and lignocellulosic biomass to liquid fuel: The influence of technical and reaction kinetic parameters. *Arabian Journal of Chemistry*. 14(4): 103035.
- Han, B, Chen, Y, Wu, Y and Hua, D. 2014. Co-pyrolysis behaviors and kinetics of plastics - biomass blends through thermogravimetric analysis Co-pyrolysis behaviors and kinetics of plastics - biomass blends through thermogravimetric analysis. July 2016.
- Hasan, A, Kong, L, Lu, W, Dejam, M and Adidharma, H. 2019. Bioresource Technology Kinetics , thermodynamics , and physical characterization of corn stover (Zea mays) for solar biomass pyrolysis potential analysis. *Bioresource Technology*. 284: 466–473.
- Li, D, Lei, S, Wang, P, Zhong, L, Ma, W and Chen, G. 2021. Study on the pyrolysis behaviors of mixed waste plastics. *Renewable Energy*. 173: 662–674. <https://doi.org/10.1016/j.renene.2021.04.035>
- Ozsin, G. 2018. A comparative study on co-pyrolysis of lignocellulosic biomass with polyethylene terephthalate , polystyrene , and polyvinyl chloride: Synergistic effects and product characteristics. 205: 1127–1138.
- Reactor, B, Growth, S, Using, R, Inoculation, E and Syahidah, R. 2016. *Improvement of bio-oil yield and quality in co-pyrolysis of corncobs and high-density polyethylene in a fixed bed reactor at a low heating rate*.
- Singh, B, Singh, S and Kumar, P. 2021. In-depth analyses of kinetics , thermodynamics, and solid reaction mechanism for pyrolysis of hazardous petroleum sludge based on isoconversional models for its energy potential. *Process Safety and Environmental Protection*. 146: 85–94.
- Stančin, H, Šafář, M, Růžicková, J, Mikulčić, H, Raclavská, H, Wang, X and Duić, N. 2021. Co-pyrolysis and synergistic effect analysis of biomass sawdust and polystyrene mixtures for production of high-quality bio-oils. *Process Safety and Environmental Protection*. 145: 1–11. <https://doi.org/10.1016/j.psep.2020.07.023>
- Teshome, FB. 2021. Municipal solid waste management in Ethiopia; the gaps and ways for improvement. *Journal of Material Cycles and Waste Management*. 23(1): 18–31. h
- Wang, X, Jin, Q, Wang, L, Bai, S, Mikulčić, H, Vujanović, M and Tan, H. 2019. Synergistic effect of biomass and polyurethane waste co-pyrolysis on soot formation at high temperatures. *Journal of Environmental Management*. 239: 306–315. <https://doi.org/10.1016/j.jenvman.2019.03.073>
- Wang, Z, Burra, KG, Lei, T and Gupta, AK. 2021. *Co-pyrolysis of waste plastic and solid biomass for synergistic production of biofuels and chemicals-A review*. Progress in Energy and Combustion Science; Elsevier Ltd.
- Xing, X, Wang, S and Zhang, Q. 2019. Thermogravimetric analysis and kinetics of mixed combustion of waste plastics and semicoke. *Journal of Chemistry*. 2019.
- Xue, J, Zhuo, J, Liu, M, Chi, Y, Zhang, D and Yao, Q. 2017. Synergetic effect of co-pyrolysis of cellulose and PP over an all-silica mesoporous catalyst MCM-41 using TG-FTIR and Py-GC-MS. <https://doi.org/10.1021/acs.energyfuels.7b01651>
- Zhang, L, Bao, Z, Xia, S and Lu, Q. 2018. *Catalytic Pyrolysis of Biomass and Polymer Wastes*. *Catalysts*. 8(12): 659.